The Eurasia Proceedings of Science, Technology, Engineering and Mathematics (EPSTEM)
ISSN: 2602-3199

The Eurasia Proceedings of Science, Technology, Engineering and Mathematics (EPSTEM), 2026

Volume 39, Pages 30-39

IConTech 2026: International Conference on Technology

Assessment of Fracture Properties in Lime-Pumice Mortars Through the Utilization of Various Specimen Types

Ragip Ince
Firat University

Erkin Eren
Firat University

Abstract: Linear elastic fracture mechanics (LEFM) were initially applied to cementitious materials by Kaplan in 1961, followed by Kesler and his colleagues in 1972. The latter group found that LEFM was inadequate for concrete. This limitation stems from the relatively inelastic region found in quasi-brittle materials, such as concrete mixtures, rocks, and bituminous substances, which are significantly and completely fractured in advance of the crack tip. As a result, many researchers have developed non-Hookean fracture mechanics methodologies to accurately describe fracture-dominated failures in quasi-brittle structures. In this investigation, beams and single-notch cube bending (SNCB) specimens with three distinct initial crack lengths were fabricated to ascertain the fracture parameters of lime-pumice mortars. All specimens, featuring a maximum aggregate diameter of 4 mm, were maintained wrapped in stretch film within the mold for 28 days, after which they underwent three-point bending tests. The fracture parameters of the mixtures were assessed using the modified peak load method, which was recently formulated to evaluate the fracture characteristics of TPM.

Keywords: Fracture mechanics, Lime, Pumice, Two-parameter model

Introduction

The application of Linear Elastic Fracture Mechanics (LEFM) to concrete began with Kaplan in 1961. However, during the 1970s, extensive experimental studies revealed that LEFM was insufficient for cement-based materials (Kesler et al., 1972). This limitation arose from the presence of an inelastic zone characterized by large-scale and fully developed cracks at the crack tip in concrete. LEFM overlooked this fracture process zone (FPZ). Consequently, various researchers have formulated nonlinear fracture mechanics methods to effectively characterize the FPZ. Initially, computational techniques known as cohesive crack models were introduced, which simulate the FPZ by applying a closing pressure that diminishes as it approaches the crack tip (Hillerborg et al., 1976; Bazant & Oh, 1983). Following this, deterministic size effect models were proposed to explain fracture-dominated failures in concrete structures, as the length of the FPZ decreases with increasing structural size. Furthermore, effective crack models, including the two-parameter fracture model (TPM) (Jenq & Shah, 1985), the effective crack model (Nallathambi & Karihaloo, 1986) the size effect model (SEM) (Bazant & Kazemi, 1990), the double-K model (Xu & Reinhardt, 1999), and the boundary effect method (Hu & Duan, 2008), were developed to simulate the FPZ using an effective crack length.

In order to examine a concrete structure concerning fracture mechanics, it is essential to first ascertain its fracture parameters. The notched beam tests are employed initially, as beams were extensively utilized in the early LEFM test standards for metals in concrete fracture. While both beams and compact tension (CT) specimens with cracks are commonly used to assess fracture properties of quasi-brittle materials and metals, the adoption of compact specimens has recently gained traction for cementitious materials, rock, and asphalt concrete. Wedge-splitting specimens and compact compression specimens have been introduced as alternatives

- Selection and peer-review under responsibility of the Organizing Committee of the Conference

to CT specimens and are frequently utilized to evaluate the nonlinear fracture properties of cementitious composites such as mortar and concrete (Ince & Bildik, 2021). Although splitting specimens in cylindrical and cubical shapes have been widely employed to indirectly assess the tensile strength of quasi-brittle materials, their centrally notched variants have also been utilized to determine the nonlinear fracture properties of cementitious materials. Ince (2021) modeled edge-notched mortar cubes, which function as splitting specimens, using the TPM. Eren and Ince (2025) applied SNCB specimens to lime-pumice mixtures. The semi-circular bending (SCB) specimens are the most prevalent samples in fracture testing of rock and asphalt materials, as they can be easily fabricated from cylindrical core samples. Ince et al. (2024) initially established some LEFM relationships concerning crack blunting in SCB specimens and subsequently simulated various SCB tests on asphalt from the literature using the TPM in concrete fracture. Recently, Ince (2025a) carried out two series of experimental investigations with SCB and beam specimens composed of concrete and mortar, discussing the findings based on the three most recognized fracture models: the TPM, the SEM, and the double-K model. Subsequently, three sets of SCB rock tests from the literature were examined utilizing the previously mentioned concrete fracture models, highlighting that the nonlinear fracture characteristics of both rock and concrete materials can be accurately evaluated using single-sized SCB specimens. The fracture tests from comparative studies on beams and single-notch cube bending (SNCB) specimens conducted by Ince and Eren (2026) demonstrate that the fracture characteristics of rocks, as determined by the TPM and the double-K model, can be readily estimated through SNCB specimen tests, thereby negating the need for specimens of varying sizes.

In this study, beams and SNCB specimens with three different initial crack lengths were created to determine the fracture parameters of lime-pumice mortars. All specimens, which had a maximum aggregate diameter of 4 mm, were kept wrapped in stretch film inside the mold for 28 days, after which they were subjected to three-point bending tests. The fracture properties of the mortars were evaluated using the modified peak load method, a recent development aimed at assessing the fracture characteristics of TPM.

The Two-Parameter Model (TPM) in Fracture Mechanics of Cementitious Materials

TPM advises that for the fracture criteria, the stress intensity factor K_I and the crack tip opening displacement *CTOD* must attain their critical values, K^s_{Ic} and $CTOD_c$, as depicted in Figure1. These fracture parameters can be calculated using the subsequent LEFM equations:

$$K_{Ic}^{s} = \sigma_{Nc}\sqrt{\pi a_c}\,Y\left(g,l\right) \tag{1}$$

$$CTOD_c = \frac{\gamma\sigma_{Nc}a_c}{E}V_1\left(g,l\right)M\left(g,l\right) \tag{2}$$

Here, σ_{Nc} refers the nominal strength, E denotes elasticity modulus, and Y, V_1, and M are normalized functions of both the structural geometry (g) and the loading configuration (l). In Eq. (2), the coefficient γ takes the value of π for splitting specimens and 4 for beams. The term Y is commonly referred to as the geometry factor, while M is obtained from the ratio COD(a_c)/CMOD$_c$, where $CMOD_c$ corresponds to the critical crack mouth opening displacement. The TPM is particularly convenient for structural applications, since the functions Y, V_1, and M can be readily found in LEFM handbooks (Tada et al., 2000).

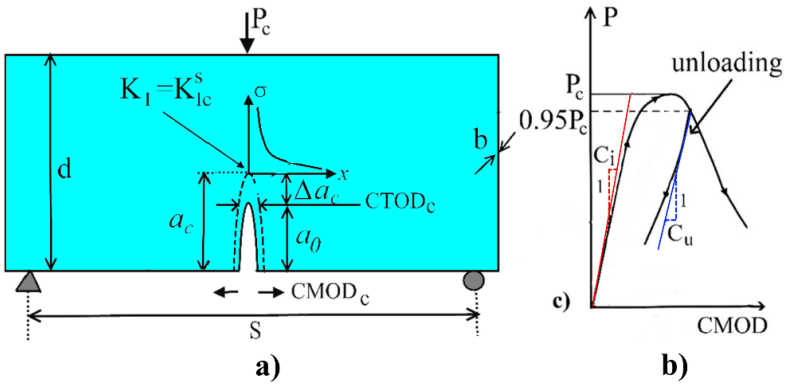

Figure 1. a) Simulation of beams based on TPM b) typical load-CMOD curve

In this methodology, the fracture parameters can be inferred from one of two distinct experimental techniques, specifically the compliance method introduced by RILEM (Shah, 1990) and the peak load method established by Tang et al. (1996). In the initial technique, these parameters are ascertained from the correlation between load and crack mouth opening displacement (P-CMOD) of three-point bending specimens featuring a central edge notch in Figure 1a, utilizing closed-loop testing apparatus. The critical crack length a_c is derived from two measurements obtained from the P-CMOD curve: the initial compliance and the unloading compliance, which is recorded at approximately 95% of the peak load during the descending phase, as shown in Figure 1b. The peak-load method, on the other hand, removes the necessity for complex closed-loop apparatus, thereby offering a more straightforward alternative to the RILEM compliance-based procedure for determining fracture parameters in TPM. However, this method still necessitates a minimum of three specimens to address the variability that is intrinsic to concrete. The test specimens can either possess the same geometrical dimensions but vary in their initial notch lengths, or they may maintain uniform notch sizes while differing in overall dimensions. For each specimen, the governing equations of TPM can be articulated as outlined by Tang et al. (1992).

$$\begin{aligned} K_I^i\left(\sigma_{Nc}^i, a_c^i\right) &= K_{Ic}^s \qquad , i = 1,2 \\ CTOD^i\left(\sigma_{Nc}^i, a_c^i\right) &= CTOD_c \end{aligned} \tag{3}$$

here i denotes the ith specimen. As a result, the parameters related to fractures can be determined by concurrently solving four non-linear equations. Nevertheless, it is essential to test three or more different specimens to guarantee statistically valid outcomes, as random errors are invariably present in the measured values of σ^1_{Nc} and σ^2_{Nc}.

Ince (2025b) has recently introduced a modified peak load method that employs an optimization procedure to determine K^s_{Ic} and $CTOD_c$. This methodology relies on the simultaneous resolution of equation (3), which serves as the failure criterion for a concrete structure. As previously stated, the primary objective of any fracture model is to assess the critical crack extension (Δa_c) at the peak load, as depicted in Figure 1a. Therefore, for this particular issue, it may be adequate to identify the nominal strength value (σ_{Nc}) that corresponds to the peak load, along with the Δa_c value for the initial crack length (a_0) for each specimen. The Δa_c values computed for each specimen should ensure that the same fracture parameters (K^s_{Ic} and $CTOD_c$) are satisfied across all tested specimens. Nevertheless, achieving an exact solution for a heterogeneous material such as concrete is unattainable. As a result, this issue can only be addressed through optimization techniques. To ascertain the fracture parameters of the TPM, the following two expressions were initially minimized by applying the least squares error criterion:

$$f\left(K_{Ic}^s\right) = \sum_{i=1}^{n} \Delta^2\left(K_{Ic}^s\right) = \sum_{i=1}^{n}\left(K_{Ic,i}^s - \overline{K_{Ic,i}^s}\right)^2 \tag{4}$$

$$f\left(CTOD_c\right) = \sum_{i=1}^{n} \Delta^2\left(CTOD_c\right) = \sum_{i=1}^{n}\left(CTOD_{c,i} - \overline{CTOD_{c,i}}\right)^2 \tag{5}$$

In which n is the number of samples experimented, $\overline{K_{Ic,i}^s}$ is the mean value of K^s_{Ic} and $K^s_{Ic,i}$ is the value of K^s_{Ic} or the i^{th} sample in Equation 4 while $\overline{CTOD_{c,i}}$ is the mean value of $CTOD_c$ and $CTOD_{ci}$ is the value of $CTOD_c$ for the i^{th} sample in Equation 5. Conversely, to achieve a simultaneous resolution of the aforementioned two minimization equations, the root sum squared (RSS) method, also referred to as the statistical tolerance analysis method, was employed as detailed below:

$$RSS = \sqrt{\left(f\left(K_{Ic}^s\right)\right)^2 + \left(f\left(CTOD_c\right)\right)^2} \tag{6}$$

It is important to recognize that while K^s_{Ic} and $CTOD_c$ are typically expressed in MPa√m and mm, respectively, it is advisable to utilize MPa√mm and μm instead, as the values represented by these units differ significantly. The aforementioned procedures, which underpin the modified peak load method, can be readily executed using a spreadsheet application like the MS-EXCEL-based SOLVER toolkit.

Experimental Program

In this study, by using CL-80-S type lime, pozzolanic activity tests of pumice material were first carried out according to TS 25 (1975). For this purpose, lime-pumice mortar was poured into cement molds (40 × 40 × 160 mm) containing three standard prismatic cavities, according to the mixing ratios recommended in TS 25 (1975). The samples were covered with hard mica material, wrapped in stretch film, and left to set for 1 day, then kept in an oven at 55°C for 1 week. Four hours before the bending test, the samples were removed from the oven and allowed to cool. Then, they were first subjected to a three-point bending test in a cement testing machine with a capacity of 30 kN and a support span of 100 mm. Six samples obtained from the three bending specimens, which were divided in two, were subjected to a compression test in a cement press with a capacity of 40 kN on a 40 × 40 mm loading area. As a result, the flexural-tensile strength of the lime-pumice mortar was obtained as 2.3 MPa > 1.0 MPa and the compressive strength as 4.4 MPa > 4.0 MPa, and it was determined that the pozzolanic activity of the pumice material conforms to TS 25 (1975).

The mixtures with a maximum aggregate diameter of 4 mm were in a water: lime: pumice: aggregate ratio of 1.53:1.00:1.00:6.00 by using two different lime types, namely CL-80-S lime with the specific gravity=2.08 and CL-90-S lime with the specific gravity=2.09. As shown in Table 1, in this study, mixtures with CL-80-S lime and with CL-90-S lime were named Mixture 1 and Mixture 2, respectively. The aggregate was air-dried prior to mixing. The Fuller parabola was used to determine the percentages of the aggregate gradation.

Beams with width × depth × length of 50×50×150 mm and square prismatic specimens with 50×150×150 mm were produced from Mixture 1, while cubes with 100 mm were produced from Mixture 2. In addition to the notched specimens, cubes (100 mm) were made to determine compressive strength. Specimens left in molds outdoors for 24 hours were then covered with stretch film and saved in the molds for 28 days. After 28 days, the modulus of elasticity was determined for the beams of Mixture 1 and the cube specimens of Mixture 2 using ultrasonic testing techniques. In this study, by using the following formulas, the dynamic modulus of elasticity of the material was determined for prismatic specimens and cubical specimens, respectively:

$$E_d = 10^3 V^2 \Delta, \quad \text{MPa} \tag{7}$$

$$E_d = 10^3 \frac{V^2 \Delta (1+\nu)(1-2\nu)}{1-\nu}, \quad \text{MPa} \tag{8}$$

where, V is the velocity (km/s) and Δ is the unit weight (kg/lt). Since lime-pumice mixtures are low strength materials, the Poisson ratio (ν) was taken as 0.3 in this study (Erdogan, 2003). Note that the dynamic modulus of elasticity of the material (E_d) are larger than the static modulus of elasticity (E_s). The formula: E_s=6/7×E_d was used for lime-pumice mixtures in this study (Lydon, 1984). Physical and mechanical properties of lime-pumice mixtures used in this study are summarized in Table 1.

The specimens were notched with a diamond saw blade of 1.5 mm thickness on the day of the fracture test. Subsequently, the compression tests and the bending tests were performed using a digital compression machine with a capacity of 100 kN. The specimens were loaded monotonically until final failure and care was taken to apply a constant loading rate (Figure 2). Typically, approximately 2 min (± 30 sec) elapsed before the maximum load capacity for each specimen was reached.

The specimen width (b), specimen depth (d) and the peak load values (P_c) of the notched beams and the SNCB specimens are reported in Table 2 and Table 3 according to the notch depths (a_0), respectively. In these tables, the letters B and S refer to beams and SNCB specimens. The following numbers in SNCB specimens in Table 3 represent the specimen size. Crack patterns at the failure of beams and compression cubes are shown in Figure 3.

Table 1. Physical and mechanical properties of lime-pumice mixtures used in this study

Mix	Lime	Δ g/cm^3	f_c MPa	E_s MPa
Mixture1	CL-80-S	1.93	3.79	13384
Mixture2	CL-90-S	2.03	3.75	12537

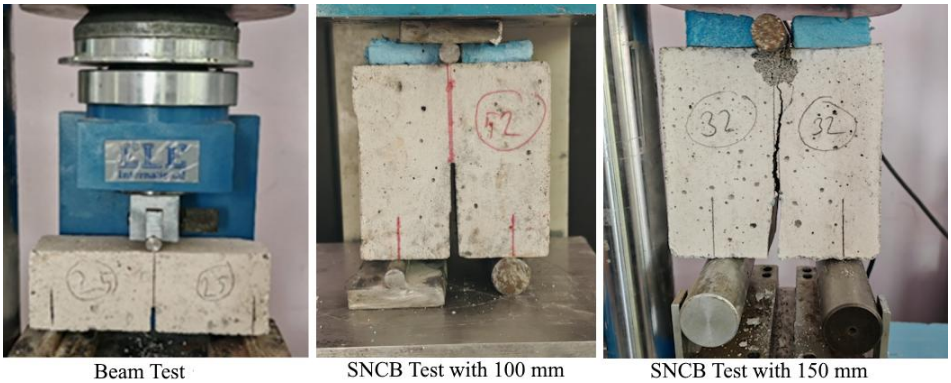

Beam Test | SNCB Test with 100 mm | SNCB Test with 150 mm

Figure 2. Test setup of the notched specimens

Figure 3. Crack patterns and failure mechanisms of notched specimens

Table 2. Test results of specimens with mixture 1 tested in this study

Specimen	b mm	d mm	a_0 mm	P_c kN	Specimen	b mm	d mm	a_0 mm	P_c N
S150-1	51.30	150.35	47.94	4.97	B1	47.77	49.32	8.84	540
S150-2	51.14	150.49	47.63	4.13	B2	50.85	50.3	9.99	460
S150-3	52.43	150.92	47.30	4.98	B3	54.16	49.63	9.71	590
S150-4	51.10	152.44	60.50	3.80	B4	50.41	50.23	9.36	680
S150-5	51.52	151.60	61.04	3.67	B5	52.08	50.41	9.93	520
S150-6	52.15	150.06	58.12	5.36	B6	53.65	50.03	15.00	350
S150-7	50.89	150.86	59.23	3.83	B7	54.26	49.84	14.26	490
S150-8	50.51	151.11	74.89	3.39	B8	49.26	50.05	13.58	410
S150-9	55.57	149.83	68.99	3.70	B9	52.21	51.28	15.79	460
S150-10	52.32	150.89	72.79	3.73	B10	52.32	50.72	15.42	450
S150-11	45.76	150.71	71.00	3.69	B11	48.02	49.63	23.12	290
					B12	50.32	49.17	21.84	250
					B13	55.85	49.21	21.43	320

Table 3. Test results of specimens with mixture 2 tested in this study

Specimen	b(mm)	d(mm)	a_0(mm)	P_c(kN)
S100-1	99.96	100.29	31.00	9.01
S100-2	99.93	99.78	30.46	9.25
S100-3	99.82	99.73	29.93	8.76
S100-4	99.94	99.34	31.48	9.52
S100-5	100.08	100.23	39.95	5.40
S100-6	99.81	99.80	50.40	5.91
S100-7	99.92	99.17	50.21	8.68
S100-8	99.94	99.80	50.42	5.32
S100-9	100.03	104.08	54.24	4.37

Applications of the Modified Peak Load Method to Lime-Pumice Mixtures

As shown in Figure 3, one of the 150 mm SNCB specimens experienced shear fracture instead of bending fracture along the crack line. Shear fracture also occurred in three of the 100 mm SNCB specimens. The most important reason for this is that SNCB specimens behave like deep beams, where the depth of the compression zone is larger than that of the beam under three-point bending loading (Ince & Eren, 2026). For this reason, these four specimens were not taken into consideration in the following analysis. The modified peak load method's specific applications to mixtures in this investigation are shown in Tables 4, 5, and 6. On the other hand, the beam and SNCB specimens were also analyzed together in Table 7 since they were produced from the same mixture in Table 2 (Mixture 1). The first two columns of these tables provide a summary of the test results for each sample. For beams and SNCB specimens, the nominal strengths were calculated as $\sigma_{Nc}=3.75P/(b\times d)$ and $\sigma_{Nc}=P/(2\times b\times d)$, respectively.

Table 4. Application of the modified peak load method to SNCB specimens with mixture 1

No	a_0 mm	σ_{Nc} MPa	Δa mm	a_c mm	a_c/d	Y	K^s_{Ic} MPa√mm	V_1	$CTOD_c$ µm		$\Delta^2(K^s_{Ic})$	$\Delta^2(CTOD_c)$
1	47.94	0.322	3.85	51.79	0.344	1.236	5.08	11.95	2.41		0.2418	0.0790
2	47.63	0.268	6.85	54.48	0.362	1.273	4.47	12.30	2.89		1.2215	0.5759
3	47.30	0.315	4.28	51.58	0.342	1.231	4.93	11.90	2.50		0.4101	0.1376
4	60.50	0.244	5.24	65.74	0.431	1.470	5.15	14.24	2.46		0.1763	0.1110
5	61.04	0.235	5.64	66.68	0.440	1.501	5.10	14.55	2.52		0.2207	0.1483
6	58.12	0.342	1.64	59.76	0.398	1.365	6.41	13.19	1.68		0.6948	0.1985
7	59.23	0.249	5.13	64.36	0.427	1.454	5.16	14.08	2.46		0.1727	0.1071
8	74.89	0.222	2.28	77.17	0.511	1.814	6.27	17.91	1.56		0.4889	0.3287
9	68.99	0.222	3.86	72.85	0.486	1.692	5.69	16.57	2.03		0.0134	0.0101
10	72.79	0.236	2.14	74.93	0.497	1.742	6.31	17.12	1.55		0.5485	0.3324
11	71.00	0.268	1.44	72.44	0.481	1.667	6.73	16.30	1.37		1.3308	0.5786
						Mean	5.57	Mean	2.13	Σ	5.5195	2.6071
											RSS	6.1042

The crack extensions (Δa_c), which were considered variables in the optimization problem, were initially chosen to be 5 mm for each sample. While the function of M in Equation 2 is shown as embedded in $CTOD_c$, the normalized functions of the cracked structure, such as Y and V_1, were also reported. The MS-EXCEL-based SOLVER toolbox was used for all analyses. The minimized values in these tables are the root sum squared (RSS) values.

Table 5. Application of the modified peak load method to beam with mixture 1

No	a_0 mm	σ_{Nc} MPa	Δa mm	a_c mm	a_c/d	Y	K^s_{Ic} MPa√mm	V_1	$CTOD_c$ µm		$\Delta^2(K^s_{Ic})$	$\Delta^2(CTOD_c)$
1	8.84	0.860	4.68	13.52	0.274	0.967	5.41	1.559	2.931		0.0012	0.0008
2	9.99	0.674	6.59	16.58	0.330	1.018	4.95	1.731	3.302		0.1807	0.1171
3	9.71	0.823	4.65	14.36	0.289	0.979	5.41	1.601	2.934		0.0010	0.0007
4	9.36	1.007	2.99	12.35	0.246	0.949	5.95	1.491	2.509		0.3260	0.2029
5	9.93	0.743	5.62	15.55	0.309	0.996	5.17	1.659	3.129		0.0435	0.0286
6	15.00	0.489	6.87	21.87	0.437	1.188	4.82	2.263	3.417		0.3170	0.2093
7	14.26	0.679	4.11	18.37	0.369	1.068	5.51	1.888	2.853		0.0173	0.0113
8	13.58	0.624	5.31	18.89	0.377	1.081	5.19	1.929	3.112		0.0348	0.0231
9	15.79	0.644	3.96	19.75	0.385	1.093	5.55	1.966	2.826		0.0283	0.0180
10	15.42	0.636	4.21	19.63	0.387	1.096	5.47	1.975	2.885		0.0086	0.0056
11	23.12	0.456	2.80	25.92	0.522	1.420	5.85	3.001	2.558		0.2182	0.1617
12	21.84	0.379	4.87	26.71	0.543	1.495	5.19	3.251	3.129		0.0361	0.0285
13	21.43	0.437	3.97	25.40	0.516	1.398	5.45	2.932	2.894		0.0056	0.0043
						Mean	5.38	Mean	2.96	Σ	1.2184	0.8119
											RSS	1.44641

Table 6. Application of the modified peak load method to SNCB specimens with mixture 2

No	a_0 mm	σ_{Nc} MPa	Δa mm	a_c mm	a_c/d	Y	K^s_{Ic} MPa√mm	V_1	$CTOD_c$ µm		$\Delta^2(K^s_{Ic})$	$\Delta^2(CTOD_c)$
1	32.00	0.449	6.31	38.31	0.382	1.321	6.51	12.76	4.36		0.7420	0.4131
2	30.46	0.464	6.31	36.77	0.369	1.288	6.42	12.44	4.40		0.9094	0.4735
3	29.93	0.440	7.23	37.16	0.373	1.297	6.17	12.53	4.60		1.4549	0.7796
4	31.48	0.479	5.54	37.02	0.373	1.298	6.71	12.54	4.20		0.4412	0.2328
5	39.95	0.269	3.45	43.40	0.433	2.502	7.86	25.74	3.45		0.2414	0.0715
6	50.40	0.297	4.35	54.75	0.549	2.038	7.93	20.48	3.16		0.3083	0.3138
7	50.21	0.438	0.92	51.13	0.516	1.840	10.22	18.21	1.65		8.0825	4.2657
8	50.42	0.267	5.63	56.05	0.562	2.128	7.53	21.53	3.56		0.0243	0.0248
9	54.24	0.210	7.74	61.98	0.595	2.395	7.01	24.77	4.07		0.1295	0.1253
						Mean	7.37	Mean	3.72	Σ	12.3335	6.7001
											RSS	14.0358

Table 7. Application of the modified peak load method to beams and SNCB specimens with mixture 1

No	a_0 mm	σ_{Nc} MPa	Δa mm	a_c mm	a_c/d	Y	K^s_{Ic} MPa√mm	V_1	$CTOD_c$ µm	$\Delta^2(K^s_{Ic})$	$\Delta^2(CTOD_c)$
1	47.94	0.322	7.98	55.92	0.372	1.296	5.53	12.52	3.87	0.1631	0.0569
2	47.63	0.268	11.55	59.18	0.393	1.351	4.94	13.05	4.26	0.9891	0.3919
3	47.30	0.315	8.58	55.88	0.370	1.292	5.39	12.48	3.96	0.3040	0.1059
4	60.50	0.244	9.42	69.92	0.459	1.573	5.69	15.30	3.81	0.0629	0.0317
5	61.04	0.235	9.83	70.87	0.467	1.609	5.64	15.68	3.84	0.0875	0.0454
6	58.12	0.342	4.52	62.64	0.417	1.424	6.84	13.77	3.07	0.8137	0.3126
7	59.23	0.249	9.28	68.51	0.454	1.555	5.69	15.11	3.81	0.0613	0.0308
8	74.89	0.222	5.66	80.55	0.533	1.940	6.85	19.35	2.89	0.8416	0.5451
9	68.99	0.222	7.67	76.66	0.512	1.819	6.27	17.97	3.37	0.1125	0.0687
10	72.79	0.236	5.45	78.24	0.519	1.857	6.88	18.39	2.89	0.8831	0.5433
11	71.00	0.268	4.27	75.27	0.499	1.756	7.22	17.27	2.68	1.6568	0.9071
1	8.84	0.860	6.14	14.98	0.304	0.991	5.85	1.644	3.72	0.0084	0.0075
2	9.99	0.674	8.19	18.18	0.361	1.058	5.39	1.857	4.13	0.2982	0.2461
3	9.71	0.823	6.12	15.83	0.319	1.006	5.84	1.693	3.72	0.0094	0.0083
4	9.36	1.007	4.24	13.60	0.271	0.964	6.35	1.550	3.25	0.1663	0.1472

5	9.93	0.743	7.18	17.11	0.339	1.029	5.60	1.767	3.94		0.1107	0.0943
6	15.00	0.489	8.35	23.35	0.467	1.256	5.26	2.477	4.25		0.4568	0.3836
7	14.26	0.679	5.46	19.72	0.396	1.110	5.93	2.019	3.63		0.0000	0.0000
8	13.58	0.624	6.77	20.35	0.407	1.129	5.63	2.079	3.92		0.0947	0.0828
9	15.79	0.644	5.30	21.09	0.411	1.137	5.97	2.105	3.60		0.0008	0.0007
10	15.42	0.636	5.57	20.99	0.414	1.142	5.90	2.119	3.67		0.0016	0.0015
11	23.12	0.456	3.82	26.94	0.543	1.494	6.27	3.248	3.29		0.1123	0.1195
12	21.84	0.379	6.04	27.88	0.567	1.594	5.65	3.585	3.92		0.0805	0.0827
13	21.43	0.437	5.12	26.55	0.539	1.481	5.91	3.204	3.66		0.0010	0.0010
						Mean	5.94	Mean	3.63	Σ	7.3161	4.2146
											RSS	8.4433

The following formulas were applied to beams with a span/depth ratio of 2.5 in this study (Yang et al., 1997):

$$Y(\alpha)=\frac{1.83-1.65\alpha+4.76\alpha^2-5.3\alpha^3+2.51\alpha^4}{\sqrt{\pi}(1+2\alpha)(1-\alpha)^{3/2}} \tag{9}$$

$$V_1(\alpha)=0.65-1.88\alpha+3.02\alpha^2-2.69\alpha^3+\frac{0.68}{(1-\alpha)^2} \tag{10}$$

$$M(\alpha_0,\alpha_c)=\sqrt{\left(1-\frac{\alpha_0}{\alpha_c}\right)^2+(1.081-1.149\alpha_c)\left[\frac{\alpha_0}{\alpha_c}-\left(\frac{\alpha_0}{\alpha_c}\right)^2\right]} \tag{11}$$

For the SNCB specimens with span/depth=0.6, the LEFM formulas were given by Ince & Eren (2026):

$$Y(\alpha)=\frac{2.854-16.967\alpha+60.766\alpha^2-102.025\alpha^3+84.581\alpha^4-27.245\alpha^5}{(1+2\alpha)(1-\alpha)^{3/2}} \tag{12}$$

$$V_1(\alpha)=8.691-27.46\alpha+5.715\alpha^2+74.589\alpha^3-101.024\alpha^4+\frac{4.476}{(1-\alpha)^2} \tag{13}$$

$$M(\alpha_0,\alpha_c)=\sqrt{\left(1-\frac{\alpha_0}{\alpha_c}\right)^2+(1.007-2.747\alpha_c+2.018\alpha_c^2)\left[\frac{\alpha_0}{\alpha_c}-\left(\frac{\alpha_0}{\alpha_c}\right)^2\right]} \tag{14}$$

Conclusion

The presented work investigated the fracture behavior of lime-pumice mixtures using the modified peak load method based on the two-parameter model in fracture mechanics of concrete. The results of this study are summarized below:

When comparing Table 6 and Table 7, SNCB specimens, previously used successfully to determine the nonlinear fracture properties of rock materials, were applied to lime-pozzolan mortars for the first time in this study. Comparative analyses revealed that the results of beam and SNCB specimens produced from the same mixture were in good agreement.

Although the amount of $Ca(OH)_2$ in CL-90-S limes is approximately 10% higher than in CL-80-S lime material in practice, other chemical and physical properties are almost the same. Consequently, the fracture toughness value of lime-pumice mortar with CL-90-S is approximately 25% greater than that of mortar with CL-80-S. On the other hand, no significant difference is observed between the crack tip opening displacement values.

It is accepted that using different specimen types together in the peak-load method for concrete fracture will yield much more reliable results. One of the important results of this study shows that this use of different specimens is also valid for the modified peak-load method.

Recommendations

Further studies can come up with more reliable results by investigating various types and sizes of aggregates to verify the above findings.

Scientific Ethics Declaration

* The authors declare that the scientific ethical and legal responsibility of this article published in EPSTEM journal belongs to the authors.

Conflict of Interest

* The authors declare that they have no conflicts of interest

Acknowledgements or Notes

* This article was presented as an oral presentation at the International Conference on Technology (www.icontechno.net) held in Budapest/Hungary on February 05-08, 2026.

* This article is extracted from the second author's doctorate dissertation entitled "Investigation of Structures Produced from Historical Mortars Using Fracture Mechanics Principles", supervised by Ragip Ince.

* Erkin Eren would like to thank the Scientific and Technological Research Council of Turkey (TÜBİTAK) for supporting his doctoral education with the Domestic General Doctoral Scholarship Program (2211-A).

References

Bažant, Z. P. & Kazemi, M. T. (1990). Determination of fracture energy, process zone length, and brittleness number from size effect with application to rock and concrete. *International Journal of Fracture*, *44(2)*, 111-131.

Bažant, Z. P. & Oh, B. H. (1983). Crack band theory for fracture concrete. *Materials & Structures (RILEM)*, *16*(93), 155-157.

Erdogan, T. Y. (2003). *Concrete*. METU Press.

Eren, E. & Ince, R. (2025). Evaluation of nonlinear fracture quantities in lime-pumice mixtures. *The Eurasia Proceedings of Science, Technology, Engineering and Mathematics (EPSTEM), 38,* 672-681.

Hillerborg, A., Modeer, M., & Petersson, P. E. (1976). Analysis of crack formation and crack growth in concrete by means of fracture mechanics and finite elements. *Cement & Concrete Research*, *6*, 773-782.

Hu, X. & Duan K. (2008). Size effect and quasi-brittle fracture: the role of FPZ. *International Journal of Fracture*, *154*, 3–14.

Ince, R. & Bildik A. T. (2021). A preliminary concrete mixture design based on fracture toughness. *Materials and Structures*, *54*:11.

Ince, R. & Eren E. (2026). Utilizing cylindrical and cubical specimens with edge notch to determine size-independent fracture quantities of rock materials. *Fracture and Structural Integrity*, *75*, 435-462.

Ince, R. (2021). Utilization of splitting strips in fracture mechanics tests of quasi-brittle materials. *Archive of Applied Mechanics*, *91*, 2661–2679.

Ince, R. (2025a). Using SCB specimens to quantify nonlinear fracture characteristics in concrete and rock materials. *Engineering Fracture Mechanics*, *318*, 110951.

Ince, R. (2025b). A modified peak load method based on the two-parameter fracture model in concrete fracture. *The Eurasia Proceedings of Science, Technology, Engineering and Mathematics (EPSTEM), 36,* 141-150.

Ince, R., Yalcin, E. & Yilmaz, M. (2024). Quantifying nonlinear fracture parameters in bituminous SCB specimens: A compliance-based approach. *Case Studies in Construction Materials*, *21*, e03437.

Jenq, Y. S. & Shah, S. P. (1985). Two-parameter fracture model for concrete. *ASCE Journal of Engineering Mechanics*, *111*(10), 1227-1241.

Kaplan, M. F. (1961). Crack propagation and the fracture of concrete. *ACI Journal*, *58*(11), 591-610.

Kesler, C. E, Naus, D. J. & Lott, L. L. (1972). Fracture mechanics-its applicability to concrete. *The Society of Materials Science,* 113-124.

Lydon, F. D. (1984). *Concrete mix design*. Applied Science publishers.

Nallathambi, P. & Karihaloo, B. L. (1986). Determination of the specimen size independent fracture toughness of plain concrete. *Magazine of Concrete Research*, *38(135)*, 67-76.

Shah, S. P. (1990). Determination of fracture parameters (KsIc sand CTODc) of plain concrete using three-point bend tests. *Materials and Structures (RILEM), 23,* 457-460.

Tada, H., Paris, P. C. & Irwin, G. R. (2000). *The stress analysis of cracks handbook*, Third Edition, ASME Press.

Tang, T., Ouyang, C. & Shah, S. P. (1996). A simple method for determining material fracture parameters from peak loads. *ACI Materials Journal*, *93*(2), 143-157.

Tang, T., Shah, S. P. & Ouyang, C. (1992). Fracture mechanics and size effect of concrete in tension. *ASCE Journal of Structural Engineering*, *118*, 3169–3185.

TS 25 (1975). *Natural pozzolan (trass) for use in cement and concrete- definitions, requirements and conformity criteria*. Turkish Standard Institute. (in Turkish)

Xu, S. & Reinhardt, H. W. (1999). Determination of double-K criterion for crack propagation in quasi-brittle fracture, Part I: experimental investigation of crack propagation. *International Journal of Fracture*, *98*, 111-149.

Yang, S., Tang, T., Zollinger, D. G. & Gurjar, A. (1997). Splitting tension tests to determine concrete fracture parameters by peak–load method. *Advanced Cement Based Materials*, *5*, 18–28.

Author(s) Information

Ragip Ince
Firat University, Engineering Faculty, Elazig, Türkiye
*Contact e-mail: *rince@firat.edu.tr*
ORCID iD: https://orcid.org/0000-0002-9837-8284

Erkin Eren
Firat University, Engineering Faculty, Elazig, Türkiye
ORCID iD: https://orcid.org/0000-0001-5282-398X

*Corresponding authors contact email

To cite this article:

Ince, R., & Eren, E. (2026). Assessment of fracture properties in lime-pumice mortars through the utilization of various specimen types. *The Eurasia Proceedings of Science, Technology, Engineering and Mathematics (EPSTEM), 39,* 30-39.